Recent Results from KASCADE-Grande and LOPES

K.-H. Kampert[a*], W.D. Apel[b], J.C. Arteaga[c†], T. Asch[d], F. Badea[b], L. Bähren[e], K. Bekk[b],
M. Bertaina[f], P.L. Biermann[g], J. Blümer[bc], H. Bozdog[b], I.M. Brancus[h], M. Brüggemann[i],
P. Buchholz[i], S. Buitink[e], E. Cantoni[fj], A. Chiavassa[f], F. Cossavella[c], K. Daumiller[b], V. de Souza[c‡],
F. Di Pierro[f], P. Doll[b], M. Ender[c], R. Engel[b], J. Engler[b], H. Falcke[ek], M. Finger[b], D. Fuhrmann[a],
H. Gemmeke[d], P.L. Ghia[j], H.J. Gils[b], R. Glasstetter[a], C. Grupen[i], A. Haungs[b], D. Heck[b],
J.R. Hörandel[e], A. Horneffer[e], T. Huege[b], P.G. Isar[b], D. Kang[c], D. Kickelbick[i], H.O. Klages[b],
Y. Kolotaev[i], O. Krömer[d], J. Kuijpers[e], S. Lafebre[e], K. Link[c], P. Łuczak[l], M. Ludwig[c], H.J. Mathes[b],
H.J. Mayer[b], J. Milke[b], M. Melissas[c], B. Mitrica[h], C. Morello[j], G. Navarra[f], S. Nehls[b], A. Nigl[e],
J. Oehlschläger[b], S. Ostapchenko[b§], S. Over[i], N. Palmieri[c], M. Petcu[h], T. Pierog[b], J. Rautenberg[a],
H. Rebel[b], M. Roth[b], A. Saftoiu[h], H. Schieler[b], A. Schmidt[d], F. Schröder[b], O. Sima[m], K. Singh[e¶],
M. Stümpert[c], G. Toma[h], G. Trinchero[j], H. Ulrich[b], W. Walkowiak[i], A. Weindl[b], J. Wochele[b],
M. Wommer[b], J. Zabierowski[l], J.A. Zensus[g]

KASCADE-Grande and LOPES Collaboration

[a]Fachbereich Physik, Universität Wuppertal, 42097 Wuppertal, Germany
[b]Institut für Kernphysik, Forschungszentrum, Karlsruhe, D-76021 Karlsruhe, Germany
[c]Institut für Experimentelle Kernphysik, Universität Karlsruhe, D-76021 Karlsruhe, Germany
[d]Inst. Prozessdatenverarb. und Elektronik, Forschungszentrum Karlsruhe, D-76021 Karlsruhe, Germany
[e]Dept. of Astrophysics, Radboud University Nijmegen, 6525 ED Nijmegen, The Netherlands
[f]Dipartimento di Fisica Generale dell'Università,10125 Torino, Italy
[g]Max-Planck-Institut für Radioastronomie, 53010 Bonn, Germany
[h]National Institute of Physics and Nuclear Engineering, P.O. Box Mg-6, RO-7690 Bucharest, Romania
[i]Fachbereich Physik, Universität Siegen, 57068 Siegen, Germany
[j]Istituto di Fisica dello Spazio Interplanetario, INAF, 10133 Torino, Italy
[k]ASTRON, 7990 AA Dwingeloo, The Netherlands
[l]Soltan Institute for Nuclear Studies, PL-90950 Lodz, Poland
[m]Department of Physics, University of Bucharest, Bucharest, Romania

KASCADE-Grande is an extensive air-shower experiment located at Forschungszentrum Karlsruhe, Germany. Main parts of the experiment are the Grande array spread over an area of 700×700 m^2, the original KASCADE array covering 200×200 m^2 with unshielded and shielded detectors, and additional muon tracking devices. This multi-detector system allows to investigate the energy spectrum, composition, and anisotropies of cosmic rays in the energy range up to 1 EeV. LOPES is co-located at the same site to measure radio pulses from extensive air showers in coincidence with KASCADE-Grande. It consists of 30 digital antennas operated in different geometrical configurations. Read out is performed at high bandwidths and rate data processing with the aim to calibrate the emitted signal in the primary energy range of $10^{16} - 10^{18}$ eV by making use of reconstructed air-shower observables of KASCADE-Grande. An overview on the performance of both experiments will be given and recent analysis results be reported.

[*]corresponding author, e-mail: kampert@uni-wuppertal.de
[†]now at: Universidad Michoacana, Morelia, Mexico
[‡]now at: U.São Paulo, Inst.de Fisica de São Carlos, Brasil
[§]now at: University of Trondheim, Norway
[¶]now at: KVI, University of Groningen, The Netherlands

1. Introduction

Even 50 years after its discovery, the origin of the 'knee' in the cosmic ray energy spectrum (a steepening of the spectrum around $4 \cdot 10^{15}$ eV) re-

mains to be understood and considerable efforts are being carried out to resolve its mystery [1]. Due to the low fluxes involved, the knee region is only accessible to large ground based experiments designed to detect extensive air showers (EAS) which are induced by primary cosmic-ray particles. Whereas this measurement method circumvents statistical problems, one has to rely on results of simulations and on the description of high energy hadronic interactions when reconstructing the properties of the primary particles. On the other hand, a thorough analysis of EAS data offers the opportunity of testing and improving the validity of these high energy interaction models.

The KASCADE-Grande experiment [2,3], located on site of the Forschungszentrum Karlsruhe (Germany), is designed to measure EAS in the energy range between 0.5 PeV and 1 EeV. The installation consists of the original KASCADE [4] experiment and the newly added Grande array, covering an effective area of $0.5\,km^2$.

The major goal of KASCADE-Grande is the observation of the 'iron-knee' in the cosmic-ray spectrum at around 100 PeV, which is expected following the KASCADE observations where the positions of the knees of individual mass groups suggest a rigidity dependence [5].

The capability of KASCADE-Grande will allow to reconstruct the energy spectra of various mass groups similar to KASCADE, which in addition will lead to hints to the energy range where the transition from cosmic rays of galactic to extragalactic origin occurs. The validity of hadronic interaction models used in CORSIKA [6] Monte Carlo simulations of ultra-high energy air showers will be also tested with KASCADE-Grande.

Investigations of the radio emission in air showers are continued at the site of KASCADE-Grande with the LOPES project [7]. It has already provided very promising results paving the way for this new detection technique. Its goals are the investigation of the relation between the radio emission from extensive air showers with the properties of the primary particles and the development of a robust, autonomous, and self-triggering antenna set-up usable for large scale applications of the radio detection technique [8,9].

In addition, within the frame of LOPES a detailed Monte-Carlo simulation program package is developed. The emission mechanism utilized in the REAS code (see [10] and references therein) is embedded in the scheme of coherent geo-synchrotron radiation. This paper sketches briefly recent results from LOPES, where the emphasis is placed on investigations of signal characteristics (lateral extension, frequency spectrum, and polarization) and of correlations of the registered radio signals with the properties of the primary cosmic particles (arrival direction and energy) by measuring in coincidence with the EAS experiment KASCADE-Grande.

2. The KASCADE-Grande Set-Up

The multi-detector experiment KASCADE (located at 49.1°n, 8.4°e, 110 m a.s.l.) [4] continues to take data since 1996. It was extended to KASCADE-Grande in 2003 by installing a large array of 37 stations consisting of $10\,m^2$ scintillation detectors each, with an average spacing of 137 m (see Fig. 1 and table 1). Each station of the so-called Grande array comprises 16 scintillators housed in individual triangular boxes and read out by photo-multipliers with a dynamic range adjusted to 1/3 to 30000 charged particles per station. The signals are amplified and shaped inside the Grande stations. After transmission to a central DAQ station digitization is done in peak sensitive ADCs. The Grande array provides an area of $0.5\,km^2$ and it operates jointly with the existing KASCADE detectors to become KASCADE-Grande.

Grande is electronically subdivided in 18 trigger clusters consisting of 7 detector stations each, one of which is indicated by the dashed lines in Fig. 1. Extensive air showers generating a 7-fold coincidence in at least one cluster will trigger the joint read-out of all Grande and KASCADE detector stations. Joint measurements with the KASCADE muon tracking devices require a fast trigger which is provided by an additional cluster (Piccolo) located nearby the center of KASCADE-Grande. Piccolo consists of $8 \times 10\,m^2$ stations equipped with plastic scintillators. Beside these Grande triggered events (0.5 Hz) the original KASCADE data acquisition
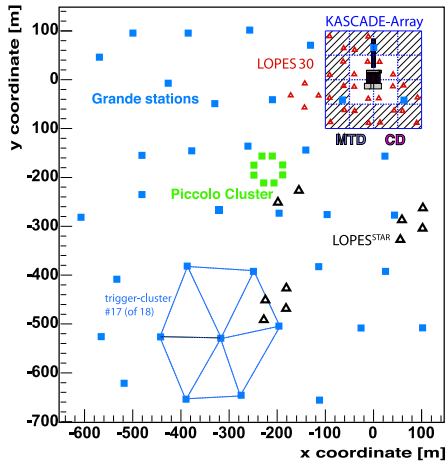
Figure 1. Layout of the KASCADE-Grande and LOPES experiment: The KASCADE array, the distribution of the 37 stations of the Grande array, the small Piccolo cluster for fast trigger purposes, and the muon tracking (MTD) and central detector (CD) are shown. The outer 12 clusters of the KASCADE array consists of μ- and e/γ-detectors, the inner 4 clusters of e/γ-detectors, only. The antennas of LOPES-30 and LOPES$^{\text{STAR}}$ are indicated by the red and blue triangles, respectively.

is continued with a trigger rate of $\approx 4\,\text{Hz}$. While the Grande detectors are sensitive to charged particles, the KASCADE array detectors measure the electromagnetic component and the muonic components separately. The muon detectors enable to reconstruct the lateral distributions of muons on an event-by-event basis also for Grande triggered events. Further muon detector systems at a Muon Tracking Detector and at the Central Detector of KASCADE (MTD and CD, respectively; see Fig. 1))allow to investigate the muon component of EAS at three different threshold energies.

3. LOPES layout and data processing

Currently, LOPES comprises 30 short dipole radio antennas (LOPES-30, Fig. 1). The antennas have been calibrated both in their absolute amplitudes and in their relative signal time [11]. In addition, LOPES runs a field of

Table 1
Compilation of the KASCADE-Grande and LOPES main detector components.

Detector Particles	sensitive area [m^2]
Grande charged	370
Piccolo charged	80
KASCADE array e/γ electrons	490
KASCADE array μ muons ($E_\mu^{\text{thresh}} = 230\,\text{MeV}$)	622
MTD muons ($E_\mu^{\text{thresh}} = 800\,\text{MeV}$)	3×128
MWPCs/LSTs muons ($E_\mu^{\text{thresh}} = 2.4\,\text{GeV}$)	3×129
LOPES 30 short dipole antennas LOPES$^{\text{STAR}}$ LPDA antennas radio emission	$> 5 \cdot 10^5$

logarithmic-dipole-antennas (LPDA) which are optimized for an application at the Pierre-Auger-Observatory and for developing a self-trigger system (LOPES$^{\text{STAR}}$ [9]). All the antennas operate in the frequency range of $40-80\,\text{MHz}$. The readout window for each LOPES-30 antenna is $0.8\,\text{ms}$ wide, centered around the trigger received from KASCADE. The sampling rate is $80\,\text{MHz}$.

The LOPES-30 data processing includes several steps [12]. First, the relative instrumental delays are corrected using a known TV transmitter visible in the data. Next, the digital filtering, gain corrections, and corrections of the trigger delays based on the known shower direction (from KASCADE) are applied and noisy antennas are flagged. Then, a time shift of the data is applied and the combination of the data is performed calculating the resulting beam from all antennas. This digital beam forming allows to place a narrow antenna beam in the direction of the cosmic ray event. To form the beam from the time shifted data, the data from each pair of antennas is multiplied time-bin by time-bin, the resulting values are averaged, and then the square root is taken while preserving the sign re-

sulting in the so-called CC-beam. Finally, there is a quantification of the radio shower parameters by fitting a Gaussian to the smoothed data. The obtained field strength ϵ is the peak height of the Gaussian divided by the effective bandwidth. Finaly, this value is compared with shower observables from KASCADE-Grande, e.g. the angle of the shower axis with respect to the geomagnetic field, the electron or muon content of the shower, the estimated primary energy, etc.

4. Update on KASCADE data analysis

The data of KASCADE have been used in a composition analysis showing the knee at 3–5 PeV to be caused by a steepening in the light-element spectra [5]. Since the applied unfolding analysis depends crucially on simulations of air showers, different high energy hadronic interaction models (QGSJet [13] and SIBYLL [14]) were used. The results have shown a strong dependence of the relative abundance of the individual mass groups on the underlying model. In a recent update of the analysis we applied the unfolding method with a different low energy interaction model (FLUKA [15] instead of GHEISHA [16]) in the simulations. While the resulting individual mass group spectra do not change significantly, the overall description of the measured data improves by using the FLUKA model [17]. In addition, data in a larger range of zenith angle were analyzed. The new results are completely consistent, i.e. there is no hint to any severe problem in applying the unfolding analysis method to KASCADE data [17].

KASCADE allows to correlate various observables of the electromagnetic, muonic, and hadronic component which is used for detailed consistency tests of hadronic interaction models. Recently [18], predictions of air-shower simulations using the hadronic interaction model EPOS 1.61 have been investigated revealing that the predictions of EPOS are not compatible with KASCADE measurements. Most likely, EPOS does not deliver enough hadronic energy to the observation level and the energy per hadron seems to be too small. By that, the number of particles at ground are shifted to lower electron and higher
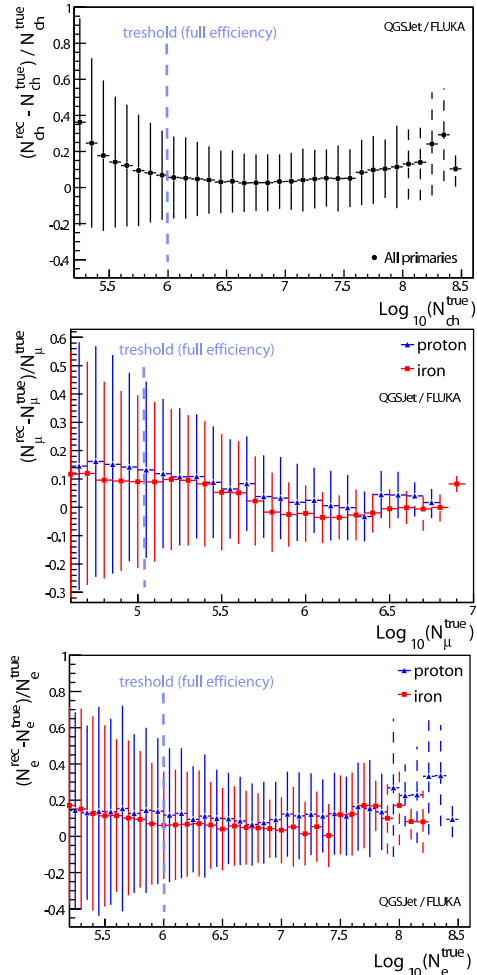

Figure 2. Charge particle, muon number, and electron number reconstruction resolution of KASCADE-Grande.

muon numbers relative to QGSJET, for example. As a consequence of this, the mass composition of cosmic rays derived by employing this model is much lighter than that obtained from QGSJet or SIBYLL.

5. Performance of KASCADE-Grande

Basic shower observables like the core position, angle-of-incidence, and total number of charged particles are provided by the measurements of the Grande stations [19,20]. A core position resolution of $\approx 10\,\mathrm{m}$, a direction resolution of
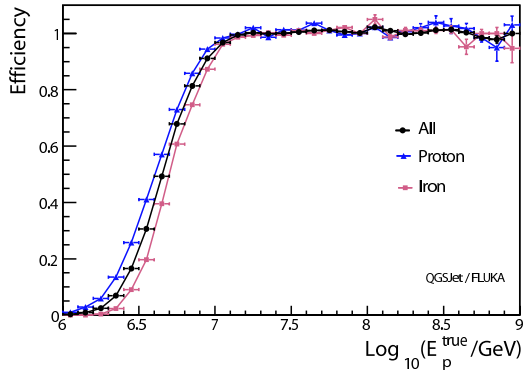
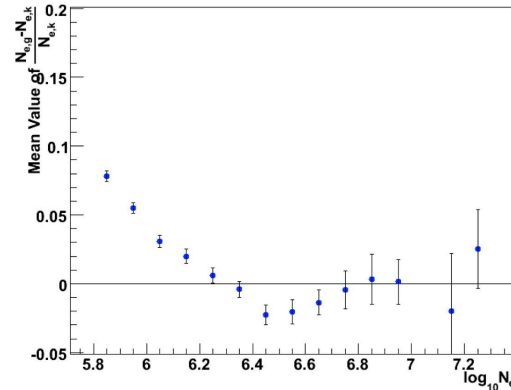Figure 3. Reconstruction and Trigger Efficiency of KASCADE-Grande.

Figure 4. Systematic difference of the shower size obtained by the Grande and KASCADE arrays. The latter one is considered as the reference [19].
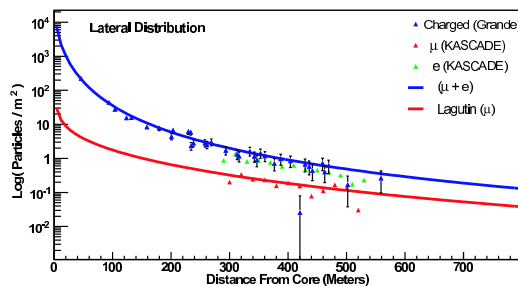

Figure 5. Example of the lateral distribution measured for a single event by the KASCADE-Grande experiment.

$\approx 0.7°$, and a resolution of the total particle number in the showers of $\approx 10\%$ is reached (see Fig. 2). The total number of muons is calculated using the core position determined by the Grande array and the muon densities measured by the KASCADE muon array detectors. In particular, this possibility to reconstruct the total muon number for Grande measured showers with a resolution $\sigma(N_\mu) \approx 20\%$ (Fig. 2) is the salient feature of KASCADE-Grande compared to other experiments in this energy range. In addition, a common fit to the energy deposits with the relative muon to electron ratio as an additional free parameter enables an estimate of the total electron number with a resolution in the order of 15% (Fig. 2).

Full efficiency for triggering and reconstruction of air showers is reached at primary energy of $\approx 2 \cdot 10^{16}$ eV (see Fig. 3).

These main characteristics of the experiment are studied with detailed CORSIKA simulations including the full simulation of the detector responses to the incident particles. In addition to Monte Carlo simulations the precisions of the reconstruction is also evaluated exploiting the unique feature of the KASCADE-Grande experiment of having two independent samplings of the same event by the KASCADE and the Grande arrays. Selecting showers with the core located in a region accessible for both arrays provides a set of events that can independently be reconstructed by both arrays. The comparison of the Grande re-

sults to those obtained by the KASCADE array confirm the simulated accuracies rather well, as can be seen e.g. in Fig. 4 [19].

An example of the particle densities of a single event is shown in Fig. 5. The particle densities measured by Grande detectors are those sampled by each single station, while for the KASCADE array the mean densities calculated in 20 m intervals of the core distance are shown. Another example of the reconstruction showing the good performance of the Grande measurements is shown in Fig. 6, where average lateral distributions of the charged particle densities for vertical EAS in different intervals of the reconstructed shower size are displayed.
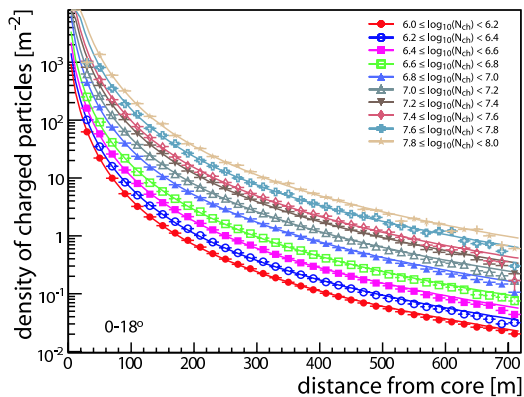
Additional sensitivity for composition esti-

Figure 6. Measured average lateral distributions of the charged particle density.

Figure 7. KASCADE-Grande shower size (total number of charged particles) spectra for different zenith angular ranges.

mates and interaction model tests is provided by muon density measurements and muon tracking at different muon energy thresholds [21]. The MTD measures the incidence angles of muons in EAS with respect to the shower axis. These radial angles provide sensitivity to the longitudinal development of the showers [22,23]. The complementary information of the showers measured by the central- and the muon tracking detectors, respectively, is predominantly being used for a better understanding of the features of an air shower and for tests and improvements of the hadronic interaction models underlying the analyses.

6. First Analyses of KASCADE-Grande

In the following, some examples are given for first analyses based on the presently available data set of KASCADE-Grande.

The estimation of energy and mass of the primary particles will be based on a combined investigation of the charged particle, electron, and muon components measured by the detector arrays of Grande and KASCADE.

Figure 7 presents the differential shower size spectra for various zenith angular ranges, where the shower size stands for the number of charged particles. These spectra will be the basis for the reconstruction of the all-particle energy spectrum of cosmic rays. The idea is to apply the constant intensity cut method (equal intensity in different zenith angular ranges means equal energy) to cor-
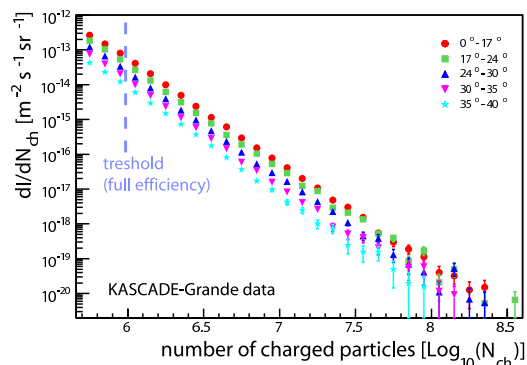
rect for the attenuation of the shower size with increasing zenith angle. In a next step, the conversion of shower size to primary energy is done by using Monte Carlo simulations for only one specific zenith angle [24].

In addition to the total number of charged particles for each event, also the total muon number (N_μ) [25] and the particle density at $500\,\mathrm{m}$ core distance ($S(500)$) [26] is reconstructed and the according spectra determined. Applying the same reconstruction method, the obtained all-particle energy spectra will be compared for cross-checks, for studies of methodical systematic uncertainties and for testing the validity of the underlying hadronic interaction model.

The total muon number measured by KASCADE-Grande allows to reconstruct also the muon density at a certain distance to the shower core. This yields sensitivity to changes in the elemental composition [27] and enables tests of hadronic interaction models.

Fig. 8 displays the measured lateral muon densities distribution for one bin in shower size and compares it with expectations for primary iron and protons in the same shower size range for two interaction models. This example resembles the results of Ref. [18] and shows that there is a large discrepancy in the available models which hampers a simple estimate of mass composition. Correlation of many observables and detailed crosschecks of the models will help to solve the three-
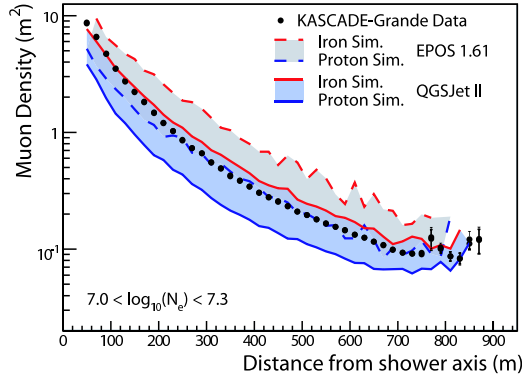
Figure 8. Example of a measured muon lateral distribution compared with predictions for two primaries by two hadronic interaction models.
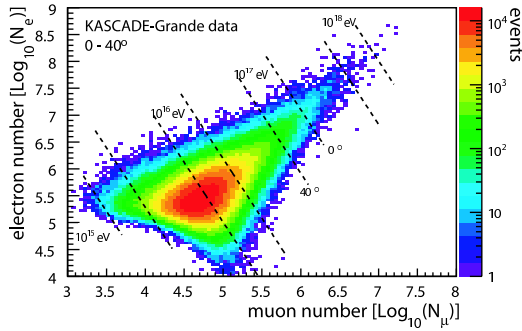

Figure 9. Two dimensional shower size spectrum of the KASCADE-Grande experiment.

fold problem of the reconstruction of the unknown primary energy, the primary mass, and to quantify the characteristics of the hadronic interactions in the air-shower development.

In the analysis of the KASCADE data, the two-dimensional distribution shower size vs. number of muons played the fundamental rôle in the reconstruction of energy spectra of single mass groups. In Fig. 9, the two dimensional shower size spectrum of electron number vs. muon number reconstructed by KASCADE-Grande is displayed. This illustrates the capability of the experiment to perform an unfolding procedure like in KASCADE.
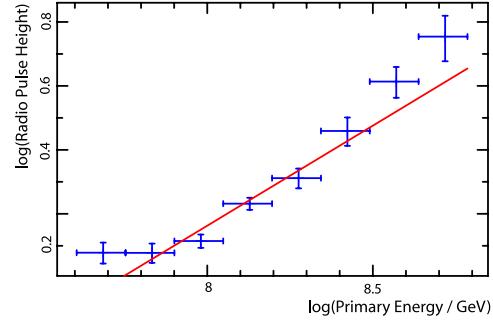

Figure 10. Average radio pulse height plotted versus the estimated primary particle energy [28].

7. Correlation of radio signals with primary energy

An important step in understanding the data provided by the radio antenna field of LOPES-30 is a study of the correlation of the radio pulse height (CC-beam) with the primary particle energy calculated from KASCADE-Grande. The fits of the dependencies of averaged pulse heights with the EAS parameters geomagnetic angle, distance to the shower axis, and primary energy are performed iteratively and results in specific relations [28], e.g. with the primary energy to $\epsilon_{EW}/[\mu V/m/MHz] \propto (E_p/10^{17} eV)^{(0.95 \pm 0.04)}$, as show in Fig. 10. The observed power-law relation yields an index close to one, i.e. a linear dependence of the field strength with the primary energy. This results serves as a proof of the coherence of the radio emission during the shower development.

8. Correlation with the geomagnetic field

A clear correlation of the pulse height with the geomagnetic angle (angle between shower axis and geomagnetic field direction) was also found indicating a geomagnetic origin of the emission mechanisms (Fig. 11). One issue that has to be kept in mind is that this analysis is only made with the east-west polarized component, which can be the reason for the debatable functional form $(1 - \cos\alpha)$ of the correlation.
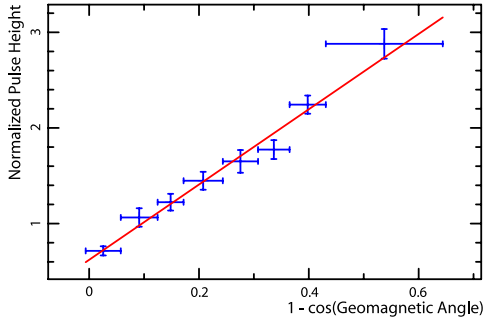
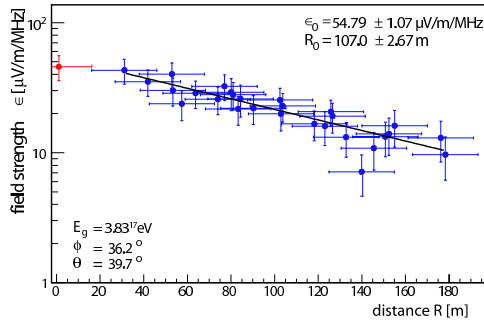Figure 11. Averaged radio pulse height plotted versus the the angle to the geomagnetic field [28].

Figure 12. Lateral distribution reconstructed from single antenna signal, shown for an individual shower [29].

9. Lateral extension of the radio signal

For the analysis of lateral distributions of the radio emission in individual events, showers with a high signal-to-noise ratio were selected, and an exponential function $\epsilon = \epsilon_0 \cdot \exp\left(-R/R_0\right)$ was used to describe the field strengths measured by individual antennas. The fit contains two free parameters, with the scale parameter R_0 describing the lateral profile and ϵ_0 the extrapolated field strength at the shower axis at observation level (example event see Fig. 12).

The distribution of the obtained lateral scale parameters peaks at $R_0 \approx 125$ m but has a tail to very large values of $R_0 > 1000\,\mathrm{m}$. Roughly, 10% of the investigated showers show very flat lateral distributions with very large scale parameters. This remarkable experimental finding is not yet understood and requires further investi-
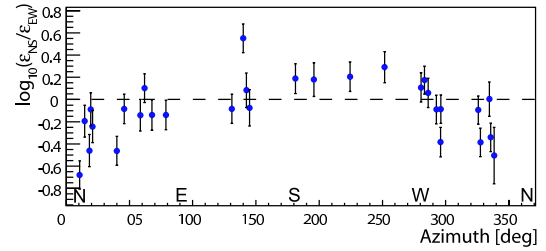

Figure 13. Pulse height ratio (North-South polarization component divided by East-West polarization component) vs. azimuth angle [20].

gations with higher statistics. The field strength ϵ_0 yields in almost all cases reliable values, i.e. they represent the above mentioned linear behavior with the primary energy.

10. Polarization characteristics

After measurements of the lateral behavior of the signal of the east-west polarization component by all 30 antennas, the LOPES-30 set-up was reconfigured to perform dual-polarization measurements. Half of the antennas have been reconfigured for measurements of the north-south polarization direction. First measurements [30] indicate a dependency of the CC-beam ratio (North-South polarization pulse height divided by the East-West pulse height) with the azimuth angle of the arriving primary particle. This is depicted in Fig. 13, where the ratio $\log \epsilon_{NS} / \log \epsilon_{EW}$ is plotted. The North-South polarization component is dominant for showers arriving from South while the East-West polarization component is dominant for showers arriving from North. This again hints to a geomagnetic origin of the emission mechanism.

11. Frequency spectrum

For a sample of a few strong events, the radio frequency spectrum received from cosmic-ray air showers in the east-west polarization direction over a frequency band of 40 MHz could be analyzed. The radio data are digitally beam-formed before the spectra are determined by sub-band filtering [31]. The resulting electric field spectra fall
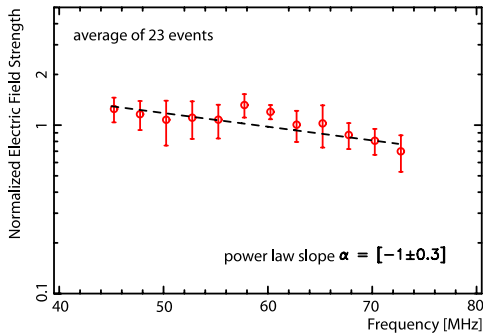
Figure 14. Comparison of average cosmic-ray electric field spectra obtained with 23 LOPES events. The frequency bin values determined on the CC-beam are fitted with a power law function (dashed line) [31].

off to higher frequencies for all individual events. But, the spectral slopes depend on the length of the pulse, where longer pulses result in steeper spectra. However, the spectra do not show a significant dependence on the electric field amplitude, the azimuth angle, the zenith angle, the curvature radius, nor on the average distance of the antennas to the shower core positions. The average frequency spectrum of the investigated events is shown in Fig. 14.

12. Summary and Conclusions

The complex KASCADE, KASCADE-Grande, and LOPES installations being operated in parallel at the same site provide unique conditions for high quality EAS measurements in the EeV-PeV energy range and for exploring the potential for future radio antenna arrays as a possible substitute or complement for present EAS observation techniques.

KASCADE-Grande is shown to be fully efficient at energies above $2 \cdot 10^{16}$ eV, thus providing a large overlap with the KASCADE energy range ($\sim 5 \cdot 10^{14}$-10^{17} eV). The reconstruction performance provided by KASCADE-Grande confirms expectations from simulations and analyses of the all-particle energy spectrum are in good agreement to previous measurements. Making use of electron and muon measurements on event-by-

event basis allows to measure the composition of cosmic rays besides their energy. This is the basis for a 2-dimensional unfolding procedure performed to extract the energy spectra for individual primary mass groups. Due to the fact that similarly to KASCADE, a wealth of information on individual showers is available also for KASCADE-Grande, tests of the hadronic interaction models and anisotropy studies will be possible in addition to the reconstruction of energy spectrum and composition.

With LOPES the proof-of-principle for detection of cosmic particles by radio flashes from extensive air showers could be performed. First results obtained by correlating the observed radio field strength with shower parameters obtained by the KASCADE measurements appear to be very promising for a more detailed understanding of the emission mechanism from atmospheric showers. Most interesting results are the found quadratic dependence of the radio-power on energy, the correlation of the radio field strength with the direction of the geomagnetic field, and the exponential behavior of the lateral decrease of the field strength with a scaling parameter in the order of hundreds of meter. Large scaling radii allow us to measure the same field strength at larger distances from the shower core, which will be helpful for large scale applications of the radio detection technique. In addition, the quadratic dependence on energy will make radio detection a cost effective method for measuring air showers at the highest energies. These results place a strong supportive argument for the use of the radio technique to study the origin of high-energy cosmic rays.

10

REFERENCES

1. K.-H. Kampert, Nucl. Phys. (Proc. Suppl.) **165** (2007) 294; astro-ph/0606619
2. G. Navarra et al. - KASCADE-Grande Coll., Nucl. Instr. Meth. **A518** (2004) 207.
3. K.-H. Kampert et al - KASCADE Coll., Nucl. Phys. (Proc. Suppl.) **122** (2003) 422.
4. T. Antoni et al - KASCADE Coll., Nucl. Instr. and Meth. **A513** (2003) 490.
5. T. Antoni et al. - KASCADE Coll., Astropart. Phys. **24** (2005) 1.
6. D. Heck et al., Report FZKA 6019, Forschungszentrum Karlsruhe (1998).
7. H. Falcke et al. - LOPES coll., Nature **435** (2005) 313.
8. A. Haungs et al. - LOPES coll., J. Phys.: Conf. Series **81** (2007) 012005.
9. T. Asch et al. - LOPES coll., Proc. of 30th ICRC, Merida, Mexico 5 (2008) 1081.
10. T. Huege, R. Engel, and R. Ulrich, Astrop. Phys. **27** (2007) 392.
11. S. Nehls et al., Nucl. Instr. Meth. **A589** (2008) 350.
12. A. Horneffer et al. - LOPES coll., Int. Journ. Mod. Phys. **A21** Suppl. (2006) 168.
13. N.N. Kalmykov and S.S. Ostapchenko, Phys. Atom. Nucl. **56** (1993) 346-353.
14. R. Engel et al., Proc. 26th Int. Cosmic Ray Conf., Salt Lake City (USA) 1 (1999) 415.
15. A. Fassò et al., Proc. Monte Carlo 2000 Conf., Lisbon, 23-26 October 2000, Springer, Berlin (2001) 955.
16. H. Fesefeldt, Report PITHA-85/02, RWTH Aachen (1985).
17. W.D. Apel et al. - KASCADE Coll., Astropart. Phys. **31** (2009) 86.
18. W.D. Apel et al. - KASCADE-Grande Coll., J. Phys. G: Nucl. Part. Phys. **36** (2009) 05321.
19. A. Chiavassa et al. - KASCADE-Grande Coll., Proc. 21st Europ. Cosmic Ray Symp., Kosice (Slovakia), (2008).
20. A. Haungs et al. - KASCADE-Grande Coll., Proc. ISVHECRI Conference 2008, to be published; A. Haungs for the LOPES Coll., ibid.
21. A. Haungs et al. - KASCADE-Grande Coll., Nucl. Phys. B (Proc. Suppl.) **175+176** (2008) 162.
22. P. Doll et al. - KASCADE-Grande Coll., Proc. ISVHECRI Conference 2008, to be published.
23. J. Zabierowski et al. - KASCADE-Grande Coll., Proc. ISVHECRI Conference 2008, to be published.
24. D. Kang et al. - KASCADE-Grande Coll., Proc. CosPA, Pohang (Korea) 2008, Modern Physics Letter A (2009), in print.
25. J.C. Arteaga et al. - KASCADE-Grande Coll., Proc. ISVHECRI Conference 2008, to be published.
26. G. Toma et al. - KASCADE-Grande Coll., Proc. ISVHECRI Conference 2008, to be published.
27. V. de Souza, J. van Buren et al. - KASCADE-Grande Coll., 30th Int. Cosmic Ray Conf., Merida (Mexico) **4** (2007) 215.
28. A. Horneffer et al. - LOPES coll., Proc. of 30th ICRC, Merida (Mexico) **4** (2007) 83.
29. S. Nehls, FZKA report **7440**, Forschungszentrum Karlsruhe (2008).
30. P.G. Isar et al. - LOPES coll., Proc. of 30th ICRC, Merida (Mexico) **5** (2007) 1093.
31. A. Nigl et al. - LOPES coll., A&A **488** (2007) 807.